

FLIERS AS STAGNATION KNOTS IN PLANETARY NEBULAE

W. Steffen,¹ J. A. López,² and A. J. Lim³

RESUMEN

Presentamos un modelo alternativo para la formación de regiones rápidas de baja ionización (FLIERS, ingl. fast low-ionization emission regions) en nebulosas planetarias. El modelo reproduce muchas de las características importantes y evita los problemas de los mecanismos de colimación y formación encontrados en estudios anteriores. En este modelo, un choque de proa cóncavo se forma como resultado de un flujo de momento lineal reducido a la largo del eje de simetría del viento estelar. Los FLIERS se forman del medio *circundante* atravesado por la onda de choque. Ya que en la zona cóncava del choque de proa el material ambiental no puede fluir alejándose del eje de simetría, éste es comprimido a un objeto denso parecido a un chorro colimado o jet (que denominamos “nudo de estancamiento” o “jet de estancamiento”). En presencia de un viento estelar variable, estos nudos rebasarán la envoltura nebulosa y aparecen como FLIERS sueltos. Presentamos simulaciones hidrodinámicas en dos dimensiones de la formación y evolución inicial de los nudos de estancamiento y jets y comparamos sus propiedades dinámicas con las de los FLIERS en nebulosas planetarias.

ABSTRACT

We present an alternative model for the formation of fast low-ionization emission regions (FLIERS) in planetary nebulae. The model is able to account for many of their attendant characteristics and circumvent the problems related to the collimation/formation mechanisms found in previous studies. In this model, a concave bow-shock structure is formed as a result of a reduced momentum flow along the symmetry axis of a stellar wind. FLIERS are formed from the shocked ambient medium. Since in the concave region of the bow-shock the ambient material can not flow away from the symmetry axis, it is compressed into a dense knot of jet-like feature (which we call “stagnation knot” or “stagnation jet”). In the presence of a variable stellar wind these knots eventually overrun the expanding nebular shell and appear as detached FLIERS. We present two-dimensional hydrodynamic simulations of the formation and early evolution of stagnation knots and jets and compare their dynamical properties with those of FLIERS in planetary nebulae.

Key Words: **HYDRODYNAMICS — ISM: JETS AND OUTFLOWS — PLANETARY NEBULAE: GENERAL — STARS: POST-AGB**

1. INTRODUCTION AND MODEL DESCRIPTION

FLIERS in planetary nebulae were originally identified with the structures previously known as ansae in elliptical planetary nebulae (Aller 1941; Balick et al. 1993). Their peculiar characteristics are now recognized in a much wider variety of PNe (e.g., Guerrero, Vázquez, & López 1999; Gonçalves, Corradi, & Mampaso 2001). Their nature has resisted a consistent explanation to date. Initially, FLIERS were considered as pairs of knots located symmetrically with respect to the PN nucleus and characterized by outflow radial velocities of the order of 30–50 km s⁻¹. Ionization gradients decrease outwards from the nebular core and in some cases ‘head-tail’ morphologies are seen with the tails pointing outwards from the nucleus (see Balick et al. 1998).

However, and as pointed out by López (2000), the concept of FLIERS has been used in recent times to encompass nearly any [N II]-bright knot in the periphery of PN shells found to be traveling either with nearly null or very high radial velocity. A single model can hardly account for all the properties observed. Symmetric ejecta, shocks, recombination fronts or simply dynamical instabilities may form in the nebular rim developing dense, low ionization knots which expand with the rim. These effects have not always been distinguished. Obviously, FLIERS are only part of a much richer variety of dynamic phenomena in PNe.

Models have proliferated with varying degrees of success in explaining the observed properties of these structures. For example, ionization fronts (IF) in localized dense knots and collimated flows which produce fast knots ramming through the shell of the PN have been discussed by Balick et al. (1998). Dopita (1997) has discussed FLIERS in terms of shocks

¹Universidad de Guadalajara, México.

²Instituto de Astronomía, UNAM, Ensenada, México.

³University College London, UK.

immersed in the strongly radiative PN environment. FLIERs do not usually show a physical connection between themselves and the nebular core. This fact has to be accounted for by any collimation model. In this regard, Frank, Balick, & Livio (1996) discussed the case of a cooling wind that avoids fast reexpansion via a collimation mechanism similar to the one described by Cantó et al. (1988). In this model the wind slides along the aspherical outer shock towards the axis forming a dense, narrow jet. Alternatively, Redman & Dyson (1999) have presented a model in which FLIERs represent recombination fronts (RF) in mass-loaded jets.

On a different approach, García-Segura & López (2000) have recently developed 3D magneto-hydrodynamic models which successfully reproduce ansae-type structures by considering a shocked stellar wind carrying a toroidal magnetic field (see Różyczka & Franco, 1996) with mass-loss rates $\leq 10^{-7} M_{\odot} \text{ yr}^{-1}$. Above this limit, jet structures develop in their model. In the MHD model, and the others mentioned above, the material cooling to form FLIERs comes from the stellar wind. In this paper we elaborate on an alternative hydrodynamical model for the formation of axial, high-velocity ansae introduced by Steffen & López (2000). In this model FLIERs are formed from external gas swept-up by a fast, low-density wind plowing into the ambient medium of the PN formed from the slow dense wind of the central star during its AGB-phase. The idea of what we call “stagnation knot” was used for the first time to reproduce the large-scale structure of the giant envelope of the PN KJPN8 (Steffen & López 1998).

1.1. The Stagnation Knot Model

Instead of an isotropic fast wind from the central region of the PN, we postulate a corresponding wind with the special property of a deficiency momentum flux along the axis as compared to higher latitudes. This causes the bow-shock to become concave instead of convex near the axis (as seen from the outside). Passing through the oblique region of the concave outer shock, the ambient medium is then refracted towards the axis, instead of away from it. This material may then remain confined by the high pressure of the surrounding hot gas from the shocked fast wind. It has sufficient time to cool and be compressed to a dense knot or long jet-like feature.

If the fast stellar wind is variable, the new formed axial FLIERs may detach from the more rapidly decelerating main envelope during the time of reduced wind power. Variable PN nuclear winds have been

clearly shown to operate in cases like the Stingray Nebula (Bobrowsky et al. 1998), LMC-N66 (Peña et al. 1997) and Lo 4 (Werner et al. 1992). The momentum flux deficiency along the axis may arise from an interacting binary system, as described by Soker & Rappaport (2000). Rapidly precessing jets could produce conical outflows (Peter & Eichler 1995, and Lim 2002, these proceedings).

In this paper we shall concentrate on the dynamical and kinematical properties of the formation and initial evolution of the stagnation knots. The study of the ionization structure around the stagnation knot, taking into account the complex shock structures and the photo-ionization from the central star, is out of the scope of the present work and will be addressed in a future paper. We show here that at least three different types of structure can be produced: first, slow ansae which remain inside or near the rim of the main nebula; second, fast ansae which move a large distance out of the rim; third, very long, jet-like strings with a linear velocity increase as a function of distance from the source.

2. SIMULATIONS

In the simulations we identify the three main structures which are observed in many PNe: a high density envelope or rim of shocked gas which propagates at a few tens of kilometers per second, small knots formed by instabilities in the dense shocked envelope, which may be associated with low-ionization knots not aligned with the symmetry axis of the nebula (Dwarkadas & Balick 1998), and fast dense knots which we identify with the ansae.

The 2D hydrodynamical simulations in axisymmetry have been calculated using the *Coral* code with a 5-level binary adaptive grid (Raga et al. 1995). This code solves the equations of mass, momentum, and energy conservation using a flux-vector-splitting scheme (van Leer 1982). The non-equilibrium cooling as described in Biro, Raga, & Cantó (1995) has been used. In order to simulate the lower limits on temperature imposed by photo-ionization from the central star without explicit calculation of the photo-ionization, a lower limit of 5000 K has been kept for the temperature. The grid size at full resolution is 513×257 grid cells. The full domain has a physical size of 1×10^{18} cm by 5×10^{17} cm. The outflow was initialized on a sphere with a radius of 5×10^{16} cm.

2.1. Initial and Boundary Conditions

The main observed dynamical and structural properties, which served as a guideline for our simulations are the following: radius of the brightest sections of the nebula between 0.25 and 0.5 parsec, rim

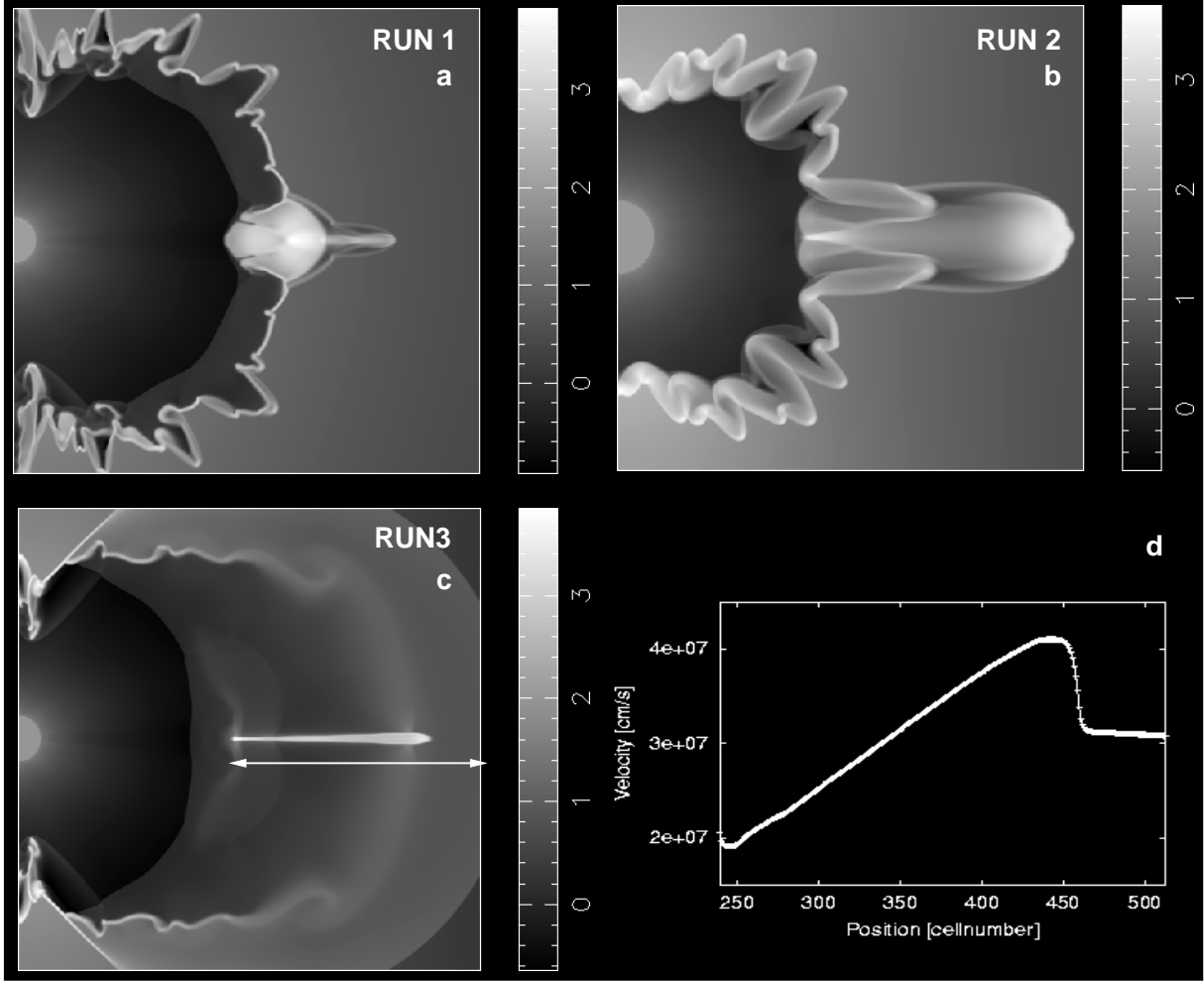


Fig. 1. Logarithmically scaled density cuts through axisymmetrical simulations are shown. (a) RUN 1, in which the stagnation knot expands significantly before escaping the rim of the PN. (b) RUN 2, in which the knot propagates about twice as far before reaching a similar expansion and has escaped the main PN. (c) RUN 3, where a “butterfly”-type PN is formed with a stagnation jet along the symmetry axis. (d) Plot of the velocity of the gas on the axis given in units of cm s^{-1} . Note the linear increase in velocity as a function of distance in the region of the dense axial jet (marked with a double arrow in panel c).

densities of order 1000 cm^{-3} with expansion speeds near 50 km s^{-1} at this size. The properties of the axial FLIERS should include a density of the order of 10^4 cm^{-3} and speeds between that of the rim and around 200 km s^{-1} , which may rise linearly with distance up to velocities over 600 km s^{-1} , as observed in the case of MyCn 18 (Bryce et al. 1997; O’Connor et al. 2000).

The initial density distribution $n(\theta)$ has been assumed to be static, varying with polar angle θ according to the equation

$$n(\theta, r) = n_0 [(1 - q) \sin^\delta \theta + q] (r/r_0)^{-\alpha}. \quad (1)$$

This distribution is equivalent to the one used by Kahn & West (1985, equation 1), except for the

free power-law parameter α . Here n_0 is the density at the fiducial distance r_0 from the star, q is the pole to equator density ratio, δ controls how fast the density rises from pole to equator. The exponent α takes into account possible deviations from the inverse square law, which might arise from time-variations of the AGB wind, which is the origin of the ambient medium.

The velocity distribution $v(\theta)$ of the fast wind,

$$\frac{v(\theta)}{v_0} = (1 - \epsilon) \sin^\kappa \left(\frac{\pi\theta}{2\theta_0} \right) + \epsilon, \quad (2)$$

has been chosen to follow the same function of polar angle as the density of the slow wind, with the difference that the maximum speed v_0 is reached at

some half opening angle θ_0 . At higher polar angles than θ_0 the wind has constant velocity. The numerical parameters κ and ϵ may of course have different values to q and δ in equation (1).

For the simulations we have used the parameters shown in Table 1.

3. RESULTS AND DISCUSSION

We have performed a series of simulations varying the following parameters: the pole-equator ratios of the velocity of the fast flow, the densities, the opening-angle of the zone of momentum depletion, and the pole-equator density ratio in the ambient medium. Figure 1 shows representative results.

As long as the central outflow is on, driving the expanding shock, the stagnation knot moves roughly at the same speed as the rest of the bow-shock and remains at the bright rim formed by shocked ambient gas. Many PNe show ansae on the rim (examples are M2-44, He1-1, NGC 6058). As soon as the outflow stops or reduces its power, the cooling envelope slows down rather quickly, whereas the dense knot continues to move at its original speed. It subsequently slows down as it expands and continues to sweep up mass from the ambient medium.

Figures 1a and 1b show stagnation knots of the slow (RUN 1) and the fast (RUN 2) types, respectively (see Table 1 for the parameters). The slow knot starts to expand significantly before it separates much from the rim of the nebula. Its speed at the time of the density image shown in Fig. 1a is around 140 km s^{-1} . The fast knot is able to reach a greater distance before it is slowed down as a consequence of its expansion. The speed of the fast stagnation knot reaches 240 km s^{-1} at the tip. The slow knot is produced in the case where there is a strong reduction of momentum along the axis (by a factor of 0.2), a relatively high ambient density along the axis and a smaller wind speed. The reverse is true for the fast knot. Here the ratio between the polar and equatorial momentum flux is only moderate (around 0.5). Densities in the stagnation knots vary roughly between 10^3 and 10^4 cm^{-3} .

Figure 1c (RUN 3) shows a very long stagnation knot or jet. Its nature is, however, different from that of jets from young stellar objects or active galaxies, which are collimated very near the central source and are refueled for the duration of the jet injection. In the stagnation knots, we have *swept-up* material which is not replaced from the central source. The most important parameters for the production of such a long jet are a small opening angle of the region of reduced momentum flow and a large pole-equator density ratio in the environment.

TABLE 1
MODEL PARAMETERS FOR THE RUNS
DISCUSSED IN THE TEXT^a

	Units	RUN 1	RUN 2	RUN 3
Wind parameters				
v_0	km s^{-1}	1000	700	1000
n_0	cm^{-3}	50	50	50
ϵ		0.5	0.2	0.5
κ		2	2	2
θ_0	$^\circ$	50	30	20
Envelope parameters				
n_0	cm^{-3}	4000	2000	3500
r_0	10^{16} cm	8	5	5
q		0.2	0.5	0.2
δ		4	4	4
α		1.95	1.95	1.95
Time	years	1190	1164	604

^aThe cut-off time of the stellar wind is 4×10^9 sec in all cases.

Three-dimensional calculations show that the formation of stagnation knots is not a consequence of the symmetry imposed in the axisymmetric calculations. In 3D, the knots form and develop in a very similar fashion to the 2D simulations (Steffen, López, & Lim 2001).

We find that in the stagnation "jets" and groups of knots, the velocity increases linearly with distance (see inset of Figure 2b). This velocity structure is very similar to that seen in the magnetohydrodynamic models of ansae developed by García-Segura, Langer, & Różyczka (1999). The accurately constant velocity gradient is established only after the full cooling of the stagnation region. Prior to full cooling, there is a noticeable increase, but it is not strictly linear. Both models, the stagnation knots and the MHD model reproduce this important observational result.

The reason for the linear velocity increase requires further investigation. Thus far, the simulations show no dependence of this self-similar velocity structure on different ambient density distributions, including constant density. Simulations of dense cylindrical slabs of gas with large-scale density gradients and small-scale velocity perturbations show that the perturbations disappear very quickly. They are dissipated as they become supersonic in the gas which reduces its sound speed as the gas cools.

If radiative cooling is insignificant, the perturbations persist as traveling waves. The large-scale gradient is slowly linearized after the cooling and during the reexpansion.

Extrapolation of the velocities, similar to the behaviour of the MHD-model, yields zero velocity before reaching the centre of the nebula. This is in contrast to the observations of the best example measured so far, MyCn 18 (O'Connor et al. 2000). Further measurements and simulations are necessary to show whether the extrapolated position of zero velocity is a significant constraint for the models.

4. SUMMARY

We have shown that the high-velocity axial FLIERs found in some bipolar planetary nebulae could be due to a reduced momentum flow along the axis of the fast stellar wind which interacts with the ambient medium. This wind configuration produces high density knots or jet-like features in the stagnation region of an initially concave bow-shock. Hence, we call them stagnation knots and stagnation jets, respectively. They are formed from radiatively cooling *ambient* gas that has been swept up in the bow-shock region. We find basically three different types of stagnation features. First, those which remain on or within the rim of the PN. Second, knots which escape the rim and, third, long jet-like features which may disintegrate to form a series of knots. Low and high velocity knots can be produced with speeds of up to several hundred kilometers per second. The stagnation knots and jets show a constant positive velocity gradient with distance from the source. Both the magnitude and the velocity gradients are consistent with observations.

W.S. is grateful for travel support from project DGAPA-UNAM IN114199 and University College London visiting researchers programme. J.A.L. acknowledges support from project DGAPA-UNAM IN114199. A.J.L. acknowledges a PPARC research associateship. We thank G. García-Segura and A. Raga for useful discussions.

W. Steffen: Instituto de Astronomía y Meteorología, Universidad de Guadalajara, Av. Vallarta 2602, 45130 Guadalajara, Jalisco, México (wsteffen@cencar.udg.mx).

J. A. López, Instituto de Astronomía, Universidad Nacional Autónoma de México, Apartado Postal 877, 22800 Ensenada, B.C., México (jal@astro.unam.mx).

A. J. Lim, Department of Physics and Astronomy, University College London, Gower Street, London WC1E 6BT, UK (ajl@star.ucl.ac.uk).

REFERENCES

- Aller, L. H. 1941, ApJ, 93, 236
 Balick, B., Alexander, J., Hajian, A. R., Terzian, Y., Perinotto, M., & Patriarchi, P. 1998, AJ, 116, 360
 Balick, B., Rugers, M., Terzian, Y., & Chengalur, J. N. 1993, ApJ, 411, 778
 Biro, S., Raga, A. C., & Cantó, J. 1995, MNRAS, 275, 557
 Bobrowsky, M., Sahu, K. C., Parthasarathy, M., & García-Lario, P. 1998, Nature, 392, 469
 Bryce, M., López, J. A., Holloway, A. J., & Meaburn, J. 1997, ApJ, 487, 161
 Cantó, J., Tenorio-Tagle, G., & Różyczka, M. 1988, A&A, 192, 287
 Dopita, M. A. 1997, ApJ, 485L, 41
 Dwarkadas, V. V., & Balick, B. 1998, ApJ, 497, 267
 Frank, A., Balick, B., & Livio, M. 1996, ApJ, 471L, 53
 García-Segura, G., Langer, N., & Różyczka, M. 1999, ApJ, 517, 767
 García-Segura, G., & López, J. A. 2000, ApJ, 544, 336
 Gonçalves, D. R., Corradi, R. L. M., & Mampaso, A. 2001, ApJ, 547, 302.
 Guerrero, M. A., Vázquez, R., & López, J. A. 1999, AJ, 117, 967
 Kahn, F. D. & West, K. A. 1985, MNRAS, 212, 837
 Lim, A. J. 2002, RevMexAA(SC), 13, 123 (this volume)
 López, J. A. 2000, RevMexAA(SC), 9, 201
 O'Connor, J. A., Redman, M. P., Holloway, A. J., Bryce, M., López, J. A., & Meaburn, J., 2000, ApJ, 531, 336
 Peña, M., Hamann, W.-R., Koesterke, L., Maza, J., Mendez, R. H., Peimbert, M., Ruiz, M. T., & Torres-Peimbert, S. 1997, ApJ, 491, 233
 Peter, W., & Eichler, D. 1995, ApJ, 438, 244
 Raga, A. C., Taylor, S. D., Cabrit, S., & Biro, S. 1995, MNRAS, 296, 833
 Redman, M. P., & Dyson, J. E. 1999, MNRAS, 302, L17
 Różyczka, M., & Franco, J. 1996, ApJ, 469, L127
 Soker, N., & Rappaport, S. 2000, ApJ, 538, 241
 Steffen, W., & López, A. J. 1998, ApJ, 508, 696
 ———. 2000, in ASP Conf. Ser. 199, Asymmetrical Planetary Nebulae II: From Origins to Microstructures, eds. J. H. Kastner, N. Soker, & S. Rappaport (San Francisco: ASP), 413
 Steffen, W., López, J. A., & Lim, A. 2001, ApJ, 556, 823
 van Leer, B. 1982, in Lecture Notes in Physics 170, Numerical Methods in Fluid Dynamics, ed. E. Krause, (Berlin: Springer), 507
 Werner, K., Hamann, W.-R., Heber, U., Napiwotzki, R., Rauch, T., & Wessolowski, U. 1992, A&A, 259, L69